

Additive splitting methods for the generalized nonlinear Schrödinger equation

Shalva Amiranashvili¹, Uwe Bandelow¹, Raimondas Čiegis²

submitted: November 29, 2024

¹ Weierstrass Institute
Mohrenstr. 39
10117 Berlin
Germany

E-Mail: shalva.amiranashvili@wias-berlin.de
uwe.bandelow@wias-berlin.de

² Vilnius Gediminas Technical University
Sauletekio av. 11
10223 Vilnius
Lithuania

E-Mail: raimondas.ciegis@vgtu.lt

No. 3144
Berlin 2024



2020 *Mathematics Subject Classification.* 78A40, 78A60, 91G60.

Key words and phrases. Nonlinear optics, nonlinear fibers, nonlinear Schrödinger equation, generalized nonlinear Schrödinger equation, modulation instability, four-wave mixing, spurious instabilities, splitting methods.

Edited by
Weierstraß-Institut für Angewandte Analysis und Stochastik (WIAS)
Leibniz-Institut im Forschungsverbund Berlin e. V.
Mohrenstraße 39
10117 Berlin
Germany

Fax: +49 30 20372-303
E-Mail: preprint@wias-berlin.de
World Wide Web: <http://www.wias-berlin.de/>

Additive splitting methods for the generalized nonlinear Schrödinger equation

Shalva Amiranashvili, Uwe Bandelow, Raimondas Čiegis

Abstract

Splitting methods provide an efficient approach to solving evolutionary wave equations, especially in situations where dispersive and nonlinear effects on wave propagation can be separated, as in the generalized nonlinear Schrödinger equation (GNLSE). However, such methods are explicit and can lead to numerical instabilities. We study these instabilities in the context of the GNLSE. Results previously obtained for multiplicative splitting methods are extended to additive splittings. An easy-to-use estimate of the largest possible integration step is derived and confirmed by numerical experiments.

1 Split-step methods

Split-step methods are numerical techniques that solve evolutionary equations by separating complex problems into simpler, more manageable parts. They are widely used in both engineering and scientific computing [1, 2, 3, 4, 5, 6]. The minimal example is a linear differential equation

$$\partial_z \psi = (B + A)\psi, \quad (1)$$

where the unknown vector $\psi(z)$ has n components and A, B are constant $n \times n$ matrices. The exact relation that involves the matrix exponential

$$\psi(z + h) = e^{h(B+A)}\psi(z), \quad (2)$$

is replaced by its splitting

$$\Psi(z + h) = e^{hB}e^{hA}\Psi(z). \quad (3)$$

Here $\Psi(z)$ approximates $\psi(z)$ for $h \rightarrow 0$ because for square matrices

$$e^{h(B+A)} = e^{hB}e^{hA} + O(h^2), \quad (4)$$

where h denotes the integration step.

In a general context, $\psi(z)$ belongs to an appropriate functional space and B, A denote possibly unbounded operators acting on this space. Both operators do not depend explicitly on z in what follows. The exponential $e^{h(B+A)}$ is understood as the evolution operator for the equation

$$\partial_z \psi = B(\psi) + A(\psi), \quad (5)$$

such that Eq. (2) holds by construction. In the same way, e^{hB} and e^{hA} denote the evolution operators for the reduced equations

$$\partial_z \psi = B(\psi) \quad \text{and} \quad \partial_z \psi = A(\psi). \quad (6)$$

It is assumed that the reduced equations and their evolution operators are easier to handle than Eq. (5).

1.1 Multiplicative methods

Approximation (4) is generalized in a natural way. A multiplicative splitting \mathcal{M} of order p with s stages, which then involves $2s$ real or complex splitting coefficients $a_{1 \leq n \leq s}$ and $b_{1 \leq n \leq s}$, is defined by

$$e^{h(B+A)} = \mathcal{M}(h) + O(h^{p+1}) \quad \text{with} \quad \mathcal{M}(h) = e^{b_s h B} e^{a_s h A} \dots e^{b_1 h B} e^{a_1 h A}. \quad (7)$$

The splitting coefficients are selected so that the formal Taylor expansions of $\mathcal{M}(h)$ and $e^{h(B+A)}$ coincide as prescribed, in particular $\sum_{1 \leq n \leq s} a_n = \sum_{1 \leq n \leq s} b_n = 1$. Equation (7) imposes further restrictions onto the splitting coefficients when the commutator $[A, B] = AB - BA \neq 0$. The simplest (Lie-Trotter) splitting with $s = p = 1$ is given by Eq. (4). The classical Strang splitting with $s = p = 2$ reads [7, 8]

$$e^{h(B+A)} = e^{\frac{1}{2}hA} e^{hB} e^{\frac{1}{2}hA} + O(h^3). \quad (8)$$

Here, the so-called *first same as last* property ($b_s = 0$) indicates that the number of stages is effectively reduced by 1. Another famous example with $s = p = 4$ reads

$$e^{h(B+A)} = e^{\frac{\sigma}{2}hA} e^{\sigma hB} e^{\frac{1-\sigma}{2}hA} e^{(1-2\sigma)hB} e^{\frac{1-\sigma}{2}hA} e^{\sigma hB} e^{\frac{\sigma}{2}hA} + O(h^5), \quad \sigma = \frac{2 + 2^{-1/3} + 2^{1/3}}{3}, \quad (9)$$

and is referred to as the Suzuki-Yoshida splitting [9, 10].

To get a better idea of the local error term, one transforms Eq. (7) to the equivalent form [10]

$$e^{h(B+A)+\Delta(h)} = e^{b_s h B} e^{a_s h A} \dots e^{b_1 h B} e^{a_1 h A} \quad \text{with} \quad \Delta(h) = O(h^{p+1}). \quad (10)$$

The Baker-Campbell-Hausdorff formula [3], which can be step by step applied to the product in Eq. (10), indicates that $\Delta(h)$ is a linear combination of commutators involving A and B . The leading term in $\Delta(h)$ consists of commutators of the length $p + 1$. All commutators with shorter lengths must cancel each other out, which gives a system of algebraic equations for the splitting coefficients.

When a basis set in the space of commutators is chosen, the local error can be characterized by the ℓ^2 norm of the leading term in $\Delta(h)$, where

$$\|\Delta(h)\| = \varkappa \frac{h^{p+1}}{(p+1)!} + O(h^{p+2}), \quad \varkappa = \text{const}. \quad (11)$$

The numerical value of \varkappa is used to compare splittings of the same order to each other. When Eq. (7) is satisfied on a manifold in the space of all splitting coefficients, the final choice of $a_{1 \leq n \leq s}$ and $b_{1 \leq n \leq s}$ is made in favor of the minimal \varkappa . For example, the splittings with $p = 4$ reported in [11] require $s = 6$, but have a local error which an order of magnitude smaller than that for the splitting (9). A comprehensive list of known splittings and their local errors can be found in [12].

1.2 Additive methods

Searching for more precise splittings, one naturally increases the number of stages s . If a larger set of splitting coefficients is not sufficient to increase p in Eq. (7), one can still reduce \varkappa in Eq. (11). Another option is to use multiple splittings of the form (7) and then to combine their predictions with appropriate weights. This procedure yields an additive splitting scheme.

Each multiplicative component of an additive splitting will be referred to as a thread, implying that different threads can be calculated independently on a multi-core machine before taking their weighted sum to accomplish an integration step. The simplest additive splitting is the second Strang splitting [7]

$$e^{h(B+A)} = \frac{1}{2} (e^{hB} e^{hA} + e^{hA} e^{hB}) + O(h^3). \quad (12)$$

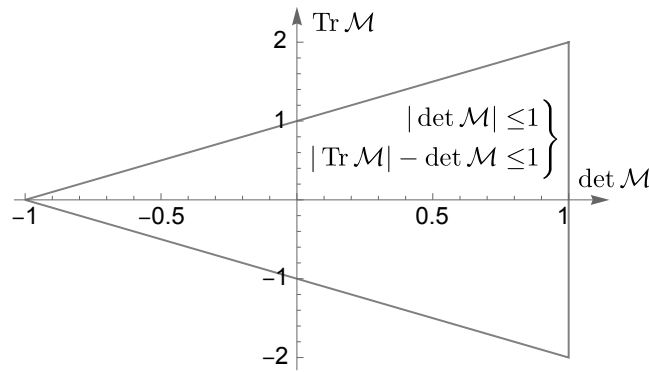


Figure 1: The stability domain for 2×2 matrix \mathcal{M} , which generates a discrete map $\mathbf{r}_{n+1} = \mathcal{M}\mathbf{r}_n$ on \mathbb{R}^2 . If the point $(\det \mathcal{M}, \text{Tr } \mathcal{M})$ is inside the triangle, the eigenvalues of \mathcal{M} are inside the unit circle. It is the root condition, e.g., see [15]. The same applies to a mapping on \mathbb{C}^2 generated by $\mathcal{U}\mathcal{M}$, where \mathcal{U} is a unitary matrix. In the area-preserving case ($\det \mathcal{M} = 1$), the root condition reduces to $|\text{Tr } \mathcal{M}| \leq 2$.

Another example is the splitting with four threads and $p = 3$ derived by Burstein and Mirin [13]

$$e^{h(B+A)} = \frac{2}{3} \left(e^{\frac{1}{2}hA} e^{hB} e^{\frac{1}{2}hA} + e^{\frac{1}{2}hB} e^{hA} e^{\frac{1}{2}hB} \right) - \frac{1}{6} (e^{hB} e^{hA} + e^{hA} e^{hB}) + O(h^4). \quad (13)$$

As a third example, we follow [14] and consider an additive splitting with four threads and $p = 4$

$$e^{h(B+A)} = \frac{2}{3} \left(e^{\frac{1}{2}hB} e^{\frac{1}{2}hA} e^{\frac{1}{2}hB} e^{\frac{1}{2}hA} + e^{\frac{1}{2}hA} e^{\frac{1}{2}hB} e^{\frac{1}{2}hA} e^{\frac{1}{2}hB} \right) - \frac{1}{6} (e^{hB} e^{hA} + e^{hA} e^{hB}) + O(h^5), \quad (14)$$

that should be compared to the Suzuki-Yoshida splitting (9). For example, the local error parameter is $\varkappa = 3.35$ for Eq. (9), it reduces to $\varkappa = 0.36$ for Eq. (14). The additive method (14) will be referred to as ARBBC splitting.

1.3 The root condition

Both multiplicative and additive splitting methods are explicit schemes, and while they are easy to implement and very fast [16, 17], they can suffer from numerical instabilities. Our goal is to study the numerical stability of the additive splitting methods (12–14) for a certain class of evolution equations. Before tackling the complete problem, it is helpful to begin with a simple toy example. Consider Eq. (1) with

$$A = \begin{bmatrix} 0 & -1 \\ 0 & 0 \end{bmatrix}, \quad B = \begin{bmatrix} 0 & 0 \\ 1 & 0 \end{bmatrix},$$

such that

$$e^{hA} = \begin{bmatrix} 1 & -h \\ 0 & 1 \end{bmatrix}, \quad e^{hB} = \begin{bmatrix} 1 & 0 \\ h & 1 \end{bmatrix}, \quad e^{h(A+B)} = \begin{bmatrix} \cos h & -\sin h \\ \sin h & \cos h \end{bmatrix}. \quad (15)$$

Equation (2) describes, for the case at hand, the rotation of a two-component vector. For any splitting method, the exact rotation matrix in Eq. (15) is approximated by a certain 2×2 matrix $\mathcal{M}(h)$. The approximation is stable when both eigenvalues of $\mathcal{M}(h)$ are inside the unit circle. This requirement imposes restrictions on $\det \mathcal{M}(h)$ and $\text{Tr } \mathcal{M}(h)$, the so-called *root condition* (Fig. 1). Table 1 shows the stability domains for the additive methods and, for comparison, for the simplest (Lie-Trotter) multiplicative method.

Equation	(4)	(12)	(13)	(14)
$\mathcal{M}(h)$	$\begin{pmatrix} 1 & -h \\ h & 1-h^2 \end{pmatrix}$	$\begin{pmatrix} 1 - \frac{h^2}{2} & -h \\ h & 1 - \frac{h^2}{2} \end{pmatrix}$	$\begin{pmatrix} 1 - \frac{h^2}{2} & -h + \frac{h^3}{6} \\ h - \frac{h^3}{6} & 1 - \frac{h^2}{2} \end{pmatrix}$	$\begin{pmatrix} 1 - \frac{h^2}{2} + \frac{h^4}{24} & -h + \frac{h^3}{6} \\ h - \frac{h^3}{6} & 1 - \frac{h^2}{2} + \frac{h^4}{24} \end{pmatrix}$
Condition	$h^2 \leq 4$	$h = 0$	$h^2 \leq 3$	$h^2 \leq 8$

Table 1: Constraints on h that guarantee that both eigenvalues of $\mathcal{M}(h)$ are inside the unit circle. We consider additive splittings, the multiplicative Lie-Trotter splitting (4) is shown for reference. The second Strang splitting (12) cannot be used. The Burstein and Mirin splitting (13) is more restrictive than the Lie-Trotter splitting but gives better accuracy. The ARBBC splitting (14) is both more accurate and less restrictive.

In what follows we will extend these results from a simple linear oscillator to a model equation that is relevant in fiber-optics. The problem breaks into an one-parametric set of two dimensional sub-problems and the root condition in Fig. 1 applies to each sub-problem. An additional difficulty is that the system in question can experience “true” instabilities that are addressed by the continuous model equations. These instabilities should be properly recovered by a splitting scheme and separated from the unwanted numerical instabilities.

2 Model equation

In the remainder of the manuscript, we will use splitting methods to describe the evolution of nonlinear dispersive waves, which are important in many physical systems [18, 19]. We assume that the waves are forced to propagate in one direction (along z axis) by the geometry of the system, like pulses in optical fibers. The wave field is given by the real part of the expression $\psi e^{i(k_0 z - \omega_0 t)}$, where k_0 and ω_0 are the carrier wave vector and circular carrier frequency, respectively. The complex envelope ψ describes wave modulations. Except for extremely short pulses, ψ evolves on a time scale much longer than $2\pi/\omega_0$, which is the slowly varying envelope approximation (SVEA).

If ψ is constant and sufficiently small, the resulting wave is linear and monochromatic. It exists only if a certain dispersion relation $k = \beta(\omega)$ is satisfied. In the vicinity of $\omega = \omega_0$, the dispersion relation is typically approximated by a polynomial, e.g., of order $J = 10$ like in [20]. Note that an envelope oscillation at the frequency Ω is translated into a field oscillation at the frequency $\omega_0 + \Omega$. The approximate dispersion law is written as

$$\beta(\omega_0 + \Omega) = k_0 + \frac{\Omega}{V_{\text{gr}}} + D(\Omega), \quad D(\Omega) = \sum_{j=2}^J \frac{\beta_j}{j!} \Omega^j, \quad (16)$$

where V_{gr} is the group velocity at carrier frequency, $D(\Omega)$ is called the dispersion function. The dispersion coefficients β_j formally refer to the derivatives $\beta^{(j)}(\omega)$ at $\omega = \omega_0$. In practice, they may be fitting parameters. The simplest nontrivial example of Eq. (16) is for $J = 2$, the parameter β_2 describes the group velocity dispersion. In an ideal material with constant index of refraction, $D(\Omega)$ vanishes.

Equation (16) cannot hold for all possible Ω , no matter how large the parameter J is [21]. In a numerical solution, however, we are always dealing with a limited bandwidth. Moreover, SVEA implies that $\Omega \ll \omega_0$ for the main part of the spectrum, in which case all pulses propagate with velocities close to V_{gr} . It is convenient to set $\psi = \psi(z, \tau)$, where $\tau = t - z/V_{\text{gr}}$ is the delay variable. The limited bandwidth refers to the Fourier transform of $\psi(z, \tau)$ with respect to τ . In the following $\tilde{\psi}(z, \Omega)$ denotes the transformed

envelope, its bandwidth is given by

$$|\Omega| \leq \Omega_N \quad \text{with} \quad \Omega_N = \frac{\pi}{\Delta\tau}, \quad (17)$$

where $\Delta\tau$ is the step size on the τ -axis and Ω_N is the circular Nyquist frequency. It is sufficient to require that Eq. (16) holds on the interval (17). In practice, only a finite number of points, say N , can be used on the τ axis. Therefore we impose a periodicity condition

$$\psi(z, \tau + T) = \psi(z, \tau) \quad \text{with} \quad \Delta\tau = T/N, \quad (18)$$

where N is also the number of harmonics after the discrete Fourier transform of the envelope. The harmonics are subject to the inequality (17) with the peculiarity that two limiting physical modes with $\Omega = \pm\Omega_N$ correspond to one discrete mode. The period T must be much larger than the temporal width of all pulses.

The evolution equation for the complex envelope ψ is derived using one or another form of multiscale expansion [22]. The result is the so-called *generalized nonlinear Schrödinger equation* (GNLSE) [23]

$$i\partial_z\psi + \sum_{j=2}^J \frac{\beta_j}{j!} (i\partial_\tau)^j \psi + \gamma|\psi|^2\psi = 0. \quad (19)$$

The γ parameter accumulates contributions by the cubic nonlinear interactions, which are assumed to be instantaneous. Equation (19) reduces to the nonlinear Schrödinger equation (NLSE) when $J = 2$.

The simplest nontrivial solution of Eq. (19) reads

$$\psi = \sqrt{P_0} e^{i\gamma P_0 z} \quad \text{with} \quad P_0 = \text{const}. \quad (20)$$

Equation (20) describes an unperturbed carrier wave with power proportional to P_0 . It is convenient to introduce the dimensionless parameter

$$\varepsilon = h\gamma P_0 \ll 1, \quad (21)$$

which will appear later in the stability analysis of the solution (20) by the numerical schemes with the evolution step h .

GNLSE (19) is a bit special because it is solved along the space variable, while the time variable serves as the coordinate. Given $\psi(z, \tau)$ at a fixed z and all τ , we want to calculate $\psi(z + h, \tau)$. For example, given the input pulse at one end of the fiber, we look for the outgoing pulse at the other end. This means, of course, that all waves propagate in the same direction and there are no reflected waves, which is a unidirectional approximation. The latter replaces SVEA in modern derivations of GNLSE-type models [24, 25, 26]. Such models get a more complex nonlinear term than in Eq. (19) and are beyond the scope of this study.

2.1 GNLSE Splitting

An important feature of Eq. (19) is that GNLSE is well suited for splitting methods. By separating linear and nonlinear terms in Eq. (19), we see that the reduced equations (6) are easy to handle. The nonlinear one has a simple analytical solution

$$\partial_z\psi = i\gamma|\psi|^2\psi \quad \Rightarrow \quad \psi(z + h, \tau) = e^{ih\gamma|\psi(z,\tau)|^2}\psi(z, \tau). \quad (22)$$

The linear one is solved by transforming $\psi(z, \tau)$ to its frequency components

$$\tilde{\psi}(z, \Omega) = \int_{-\infty}^{\infty} \psi(z, \tau) e^{i\Omega\tau} d\tau,$$

where

$$\partial_z \psi = i \sum_{j=2}^J \frac{\beta_j}{j!} (i\partial_\tau)^j \psi \Rightarrow \partial_z \tilde{\psi} = iD(\Omega) \tilde{\psi} \Rightarrow \tilde{\psi}(z+h, \Omega) = e^{ihD(\Omega)} \tilde{\psi}(z, \Omega). \quad (23)$$

Calculation of the nonlinear and linear evolution operators is then limited by the rounding errors and by the properties of the discrete Fourier transform [27].

Equations (22) and (23) are formally exact. Nevertheless, the solution of NLSE and GNLSE by splitting methods can suffer from numerical instabilities. The latter are typically weak, but can be observed at longer propagation distances, see [28]. With respect to NLSE, for example, the classical study [29] (see also [30]) established that the simplest first-order splitting (4) is stable if the evolution step h obeys the inequality

$$h \leq \frac{2\Delta\tau^2}{\pi|\beta_2|}. \quad (24)$$

These results were generalized for GNLSE in [31, 32]. An extension to the fourth-order Suzuki-Yoshida splitting (9) was reported in [33], and to an arbitrary multiplicative splitting in [34]. The extension for the additive splitting methods (12), (13), and (14) will be reported below.

2.2 Modulation instability

Following the pioneering work of Weideman and Herbst [29], the correctness of splitting methods is tested using modulation instability (MI), which is a fundamental phenomenon in the field of nonlinear waves [35]. MI occurs when small spontaneous modulations of the initially uniform carrier wave begin to grow, leading to the emergence of various localized structures, such as robust solitary pulses [36] or spontaneous rogue waves [37].

The initial stage of MI is described by considering a small perturbation of the solution (20)

$$\psi(z, \tau) = \left(\sqrt{P_0} + \xi(z, \tau) \right) e^{i\gamma P_0 z} \quad \text{with} \quad |\xi| \ll \sqrt{P_0}.$$

Equation (19) is linearized with respect to ξ , which gives

$$i\partial_z \xi + \sum_{j=2}^J \frac{\beta_j}{j!} (i\partial_\tau)^j \xi + \gamma P_0 (\xi + \xi^*) = 0. \quad (25)$$

The entire solution space of Eq. (25) can be divided into two-dimensional subspaces parameterized by the offset frequency Ω . For this, use substitution

$$\xi(z, \tau) = u(z) e^{-i\Omega\tau} + v^*(z) e^{i\Omega\tau}, \quad (26)$$

which gives a system of two coupled ODEs for each Ω

$$\partial_z \begin{bmatrix} u \\ v \end{bmatrix} = i \begin{bmatrix} D(\Omega) + \gamma P_0 & \gamma P_0 \\ -\gamma P_0 & -D(-\Omega) - \gamma P_0 \end{bmatrix} \begin{bmatrix} u \\ v \end{bmatrix}. \quad (27)$$

It is convenient to split the dispersion function into odd and even components

$$D(\Omega) = M(\Omega) + N(\Omega), \quad M(-\Omega) = M(\Omega), \quad N(-\Omega) = -N(\Omega). \quad (28)$$

The standard analysis shows that the equilibrium state $u = v = 0$ of the system (27) is unstable if [38]

$$M(\Omega) \left(M(\Omega) + 2\gamma P_0 \right) < 0. \quad (29)$$

The inequality (29) gives offsets Ω for which spontaneous growth of the perturbations (26) is expected. The offsets with the fastest growth are determined by $M(\Omega) = -\gamma P_0$, in which case u, v grow as $e^{|\gamma|P_0 z}$.

Analogous to ε from Eq. (21), it is convenient to introduce a dimensionless phase parameter

$$\phi = hM(\Omega), \quad (30)$$

where a “small” evolution step h is multiplied by a polynomial, which can take “large” values at the end of the frequency interval (17). This is a potential source of numerical instability. The main idea of the pioneer study [29] was that a correct splitting scheme should reproduce the true instability domain from Eq. (29)

$$\phi(\phi + 2\varepsilon) < 0, \quad (31)$$

while no other instabilities should appear. This idea will be applied to additive splitting schemes in the following.

2.3 Split-step framework for modulation instability

To apply Eq. (27) to the analysis of split-step methods, we must write its solution in the form (2). For this purpose, we introduce the matrix notations

$$\mathbf{I} = \begin{bmatrix} 1 & 0 \\ 0 & 1 \end{bmatrix}, \quad \mathbf{J} = \begin{bmatrix} 1 & 0 \\ 0 & -1 \end{bmatrix}, \quad \mathbf{K} = \begin{bmatrix} 1 & 1 \\ -1 & -1 \end{bmatrix}, \quad (32)$$

such that Eq. (27) takes the form

$$\partial_z \begin{bmatrix} u \\ v \end{bmatrix} = i \left(N(\Omega) \mathbf{I} + M(\Omega) \mathbf{J} + \gamma P_0 \mathbf{K} \right) \begin{bmatrix} u \\ v \end{bmatrix}.$$

For the case at hand, Eq. (2) reads

$$\begin{bmatrix} u(z+h) \\ v(z+h) \end{bmatrix} = e^{ihN(\Omega)} e^{ihM(\Omega)\mathbf{J} + ih\gamma P_0 \mathbf{K}} \begin{bmatrix} u(z) \\ v(z) \end{bmatrix}. \quad (33)$$

Note that the expressions for ε and ϕ , which were defined in advance in Eq. (21) and (30), appear naturally in Eq. (33). The stability properties of the discrete map (33) depend only on the matrix $e^{i\phi\mathbf{J} + i\varepsilon\mathbf{K}}$.

Furthermore, by separating contributions arising from linear and nonlinear terms in GNLSE (19), we see that, e.g., the simplest Lie-Trotter scheme (3) corresponds to the approximation

$$\begin{bmatrix} U(z+h) \\ V(z+h) \end{bmatrix} = e^{ihN(\Omega)} e^{i\phi\mathbf{J}} e^{i\varepsilon\mathbf{K}} \begin{bmatrix} U(z) \\ V(z) \end{bmatrix}, \quad (34)$$

where $U(z)$ and $V(z)$ denote numerical approximations to $u(z)$ and $v(z)$. This approximation is inexact because Eq. (32) gives $[\mathbf{J}, \mathbf{K}] \neq 0$.

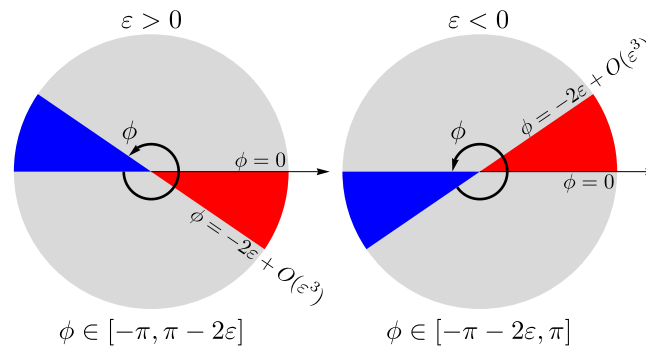


Figure 2: Given ε , inequality (37) gives two instability domains for the angle parameter ϕ . The true MI domain (31) is red, the numerical instability domain is blue. To avoid the numerical instability, we impose restrictions on ϕ , they are shown at the bottom of the figure. For simplicity, the restrictions are combined in a single sufficient condition (38).

A generic multiplicative splitting (7) gives the approximation

$$\begin{bmatrix} U(z+h) \\ V(z+h) \end{bmatrix} = e^{ihN(\Omega)} \left(\prod_{n \geq s \geq 1} e^{ib_s \phi \mathbf{J}} e^{ia_s \varepsilon \mathbf{K}} \right) \begin{bmatrix} U(z) \\ V(z) \end{bmatrix}, \quad (35)$$

and for, e.g., the second Strang splitting (12) we get

$$\begin{bmatrix} U(z+h) \\ V(z+h) \end{bmatrix} = e^{ihN(\Omega)} \left(\frac{1}{2} e^{i\phi \mathbf{J}} e^{i\varepsilon \mathbf{K}} + \frac{1}{2} e^{i\varepsilon \mathbf{K}} e^{i\phi \mathbf{J}} \right) \begin{bmatrix} U(z) \\ V(z) \end{bmatrix}. \quad (36)$$

The remaining additive splittings (13) and (14) give similar, only more cumbersome formulas. These formulas will be used in the next section to investigate the applicability of the splitting methods.

3 Applications

We are in a good position to note that the standard MI analysis, normally performed with ODEs (27), can be performed with the matrix solution (33). To this end, one calculates

$$\det(e^{i\phi \mathbf{J} + i\varepsilon \mathbf{K}}) = 1 \quad \text{and} \quad \text{Tr}(e^{i\phi \mathbf{J} + i\varepsilon \mathbf{K}}) = 2 \cos \left(\sqrt{\phi^2 + 2\varepsilon \phi} \right),$$

and applies the root condition from Fig. 1. The instability in this case occurs when

$$|\cos(\sqrt{\phi^2 + 2\varepsilon \phi})| > 1.$$

The result agrees with the MI condition (31).

Similar analysis can be done with any multiplicative or additive splitting that approximates Eq. (33). There may be several areas of instability. One should agree with Eq. (31), the others should disappear as $h \rightarrow 0$.

3.1 Lie-Trotter splitting

It is instructive to revisit the Lie-Trotter approximation [29, 30, 31, 32, 33, 34], which is described by Eq. (34) with

$$\det(e^{i\phi \mathbf{J}} e^{i\varepsilon \mathbf{K}}) = 1 \quad \text{and} \quad \text{Tr}(e^{i\phi \mathbf{J}} e^{i\varepsilon \mathbf{K}}) = 2(\cos \phi - \varepsilon \sin \phi).$$

Figure 1 shows that the instability occurs when

$$|\cos \phi - \varepsilon \sin \phi| > 1. \quad (37)$$

Considering $\varepsilon \ll 1$, the instability can be expected where $|\cos \phi| \approx 1$. Expanding Eq. (37) near $\phi = 0$, one gets the true MI domain (31). Expanding near $\phi = \pm\pi$, one gets the second domain with the numerical instability. The latter is avoided when ϕ is properly bounded, see Fig. 2.

For the simplest focusing NLSE, where $\varepsilon > 0$ and $\phi < 0$, it is sufficient to require that $|\phi| \leq \pi$. This results in Eq. (24) from Ref. [29]. In general, the even part of the dispersion function in Eq. (30) can change its sign and we impose the constraint [32]

$$|\phi| \leq \pi - 2|\varepsilon|. \quad (38)$$

It should be satisfied for any offset Ω within the total bandwidth (17). Equations (21) and (30) finally give

$$h \leq \frac{\pi}{\max_{|\Omega| \leq \Omega_N} |M(\Omega)| + 2|\gamma|P_0}.$$

This is how the largest possible integration step h appears. In practice, one can simply require

$$|\phi| \leq \pi \quad \Rightarrow \quad h \leq \frac{\pi}{\max_{|\Omega| \leq \Omega_N} |M(\Omega)|}, \quad (39)$$

and consider the result with a grain of salt. We now have everything we need to generalize Eq. (39) for the additive methods (12–14).

3.2 The second Strang splitting

The second Strang splitting (12) leads to Eq. (36), so we should study the following evolution matrix

$$\mathcal{M} = \frac{1}{2}e^{i\phi\mathbf{J}}e^{i\varepsilon\mathbf{K}} + \frac{1}{2}e^{i\varepsilon\mathbf{K}}e^{i\phi\mathbf{J}} \quad \Rightarrow \quad \begin{aligned} \det \mathcal{M} &= 1 + (\varepsilon \sin \phi)^2, \\ \text{Tr } \mathcal{M} &= 2(\cos \phi - \varepsilon \sin \phi). \end{aligned}$$

The root conditions from Fig. 1 are violated because $\det \mathcal{M} > 1$. Therefore, the second Strang splitting scheme cannot be used at all, as one would expect from the Table 1.

Consider, for example, a GNLSE with only $\beta_4 \neq 0$

$$i\partial_z\psi + \frac{\beta_4}{24}\partial_\tau^4\psi + \gamma|\psi|^2\psi = 0, \quad (40)$$

which applies to pulses in fibers with a specially managed dispersion law [39]. For what follows, it is convenient to normalize Eq. (40). We indicate the dimensionless variables by dashes and define

$$\psi' = \psi/\sqrt{P_0}, \quad z' = |\gamma|P_0z, \quad \tau' = 2\pi\tau/T, \quad (41)$$

such that the amplitude is normalized using the base solution (20), the space using the so-called *nonlinear length* $|\gamma|^{-1}P_0^{-1}$, and the delay is scaled such that $\tau' \in [-\pi, \pi]$. The normalized discrete frequencies Ω' are then integers $-N/2 \leq \Omega' < N/2$. Recall that the number of harmonics N and period T were introduced in Eq. (18). Equation (21) indicates that $h' = |\varepsilon|$.

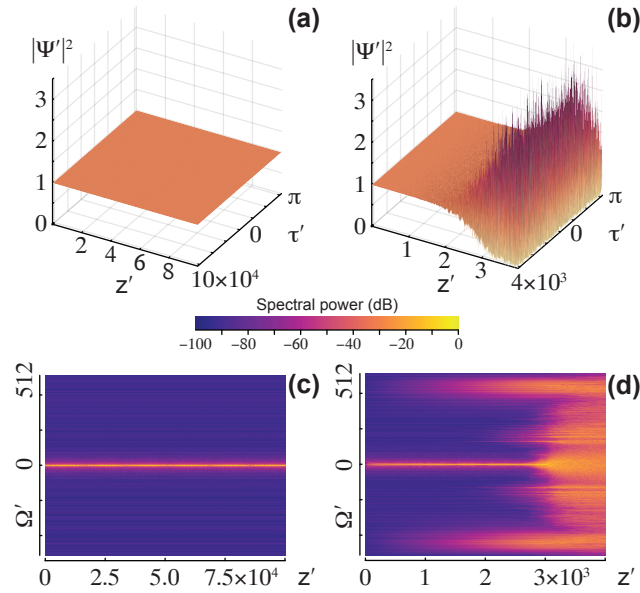


Figure 3: Normalized representation of the power $|\psi(z, \tau)|^2$ (3D plots) and the spectral power $|\tilde{\psi}(z, \Omega)|^2$ (density plots) that describes two numerical solutions of Eq. (40) for a slightly perturbed continuous wave (20) and with the same h' . The parameters are given in Eq. (42), the wave is physically stable. The solution (a,c) by the Lie-Trotter splitting is stable, because the integration step is below the limiting value (39). The solution (b,d) by second Strang splitting method is numerically unstable. A reduction in h' does not help here.

The normalized Eq. (40) depends on a single parameter $\beta'_4 = (2\pi)^4 \beta_4 / (T^4 |\gamma| P_0)$ and on the sign of γ , we assume $\gamma > 0$. The continuous wave solution (20) has the form $\psi' = e^{iz'}$. The MI condition (29) reduces to $\frac{1}{24} \beta'_4 \Omega'^4 \in (-2, 0)$, i.e., the continuous wave should be stable for $\beta'_4 > 0$. Let us check this numerically.

Figure 3 shows solutions of Eq. (40) obtained by two different splitting methods, where in both cases

$$h' = 0.005, \quad \gamma' = 1, \quad \beta'_4 = 2 \cdot 10^{-7}, \quad N = 2^{10}, \quad \psi'|_{z'=0} = 1 + (\text{random signal}), \quad (42)$$

and noise amplitude is 10^{-3} . The Lie-Trotter method is stable, see Fig. 3(a,c). Here, Eq. (39) requires $h' < 0.0055$, which is satisfied. For, e.g., $h' = 0.006$, the Lie-Trotter solution is destroyed by a numerical instability (not shown). The second Strang method is numerically unstable in any case, see Fig. 3(b,d). This instability cannot be repaired by decreasing h' .

3.3 Burstein and Mirin splitting

By analogy with Eq. (12) and (36), the Burstein and Mirin splitting (13) is related to the evolution matrix

$$\mathcal{M} = \frac{2}{3} \left(e^{\frac{i\varepsilon}{2} \mathbf{K}} e^{i\phi \mathbf{J}} e^{\frac{i\varepsilon}{2} \mathbf{K}} + e^{\frac{i\phi}{2} \mathbf{J}} e^{i\varepsilon \mathbf{K}} e^{\frac{i\phi}{2} \mathbf{J}} \right) - \frac{1}{6} \left(e^{i\phi \mathbf{J}} e^{i\varepsilon \mathbf{K}} + e^{i\varepsilon \mathbf{K}} e^{i\phi \mathbf{J}} \right),$$

with

$$\det \mathcal{M} = 1 - \frac{2\eta^2}{9} (1 + 5 \cos \phi - 4\varepsilon \sin \phi),$$

$$\text{Tr } \mathcal{M} = 2(\cos \phi - \varepsilon \sin \phi),$$

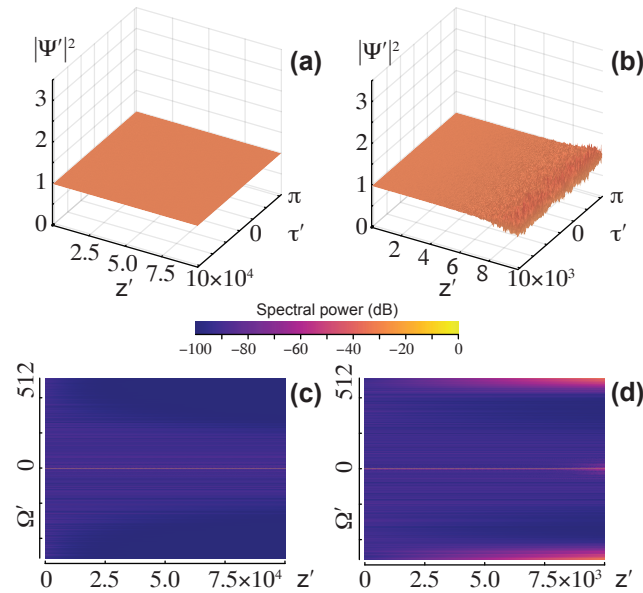


Figure 4: Normalized representation of the power $|\psi(z, \tau)|^2$ (3D plots) and the spectral power $|\tilde{\psi}(z, \Omega)|^2$ (density plots) describes two numerical solutions of Eq. (44) by the Burstein and Mirin splitting method for a physically stable continuous wave (20). The parameters are given in Eq. (45), here $\beta'_2 > 0$. Left column: the integration step $h' = 0.001$ obeys Eq. (43), the numerical solution is stable. Right column: the stability is destroyed for $h' = 0.002$.

where, for brevity, we use the notation $\eta = \varepsilon \sin(\phi/2)$. The full analysis of the root conditions from Fig. 1 is not useful here. Instead, we note that (for $|\varepsilon| < 0.25$, which is always met in practice) the root conditions are satisfied when $|\phi| \leq \pi/2$. This gives the sufficient condition

$$h \leq \frac{\pi/2}{\max_{|\Omega| \leq \Omega_N} |M(\Omega)|}, \quad (43)$$

cf. Eq. (39). Roughly speaking, the Burstein and Mirin method (13) requires a two times smaller integration step than the simplest multiplicative splitting.

Consider, for example, the standard optical NLSE [23]

$$i\partial_z \psi - \frac{\beta_2}{2} \partial_\tau^2 \psi + \gamma |\psi|^2 \psi = 0, \quad (44)$$

which we normalize following Eq. (41). The normalized NLSE depends on $\beta'_2 = (2\pi)^2 \beta_2 / (T^2 |\gamma| P_0)$ and on the sign of γ , we assume $\gamma > 0$. The MI condition (29) reduces to $\frac{1}{2} \beta'_2 \Omega'^2 \in (-2, 0)$, such that MI is expected for $\beta'_2 < 0$. Specifically, we consider the following parameters

$$\gamma' = 1, \quad \beta'_2 = \pm 0.01, \quad N = 2^{10}, \quad \psi'|_{z'=0} = 1 + (\text{random signal}), \quad (45)$$

noise amplitude is 10^{-3} . Equation (43) gives $h' < 0.0012$, we then consider $h' = 0.001$ and $h' = 0.002$.

Figure 4 uses $\beta'_2 = 0.01$, the solution (20) is then physically stable. This agrees with the numerical solution for $h' = 0.001$ in Fig. 4(a,c). For $h' = 0.002$ the wave is destroyed by the numerical instability, see Fig. 4(b,d).

Figure 5 uses $\beta'_2 = -0.01$. The onset of MI is observed in Fig. 5(a,b), which was calculated for $h' = 0.002$. This solution is destroyed by the numerical instability as z increases, see Fig. 5(c). The numerical instability is removed and MI is unaffected for $h' = 0.001$ (not shown).

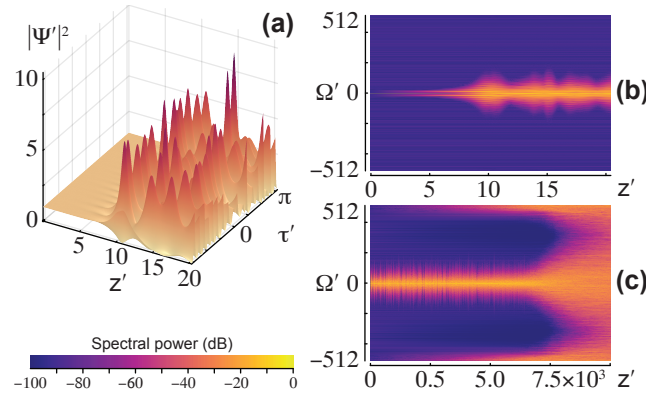


Figure 5: Normalized representation of the power $|\psi(z, \tau)|^2$ (the 3D plot) and the spectral power $|\tilde{\psi}(z, \Omega)|^2$ (density plots) that describes a numerical solution of Eq. (44) by the Burstein and Mirin splitting for an unstable continuous wave (20). The parameters are given in Eq. (45), here $\beta'_2 < 0$. The onset of MI (a,b) is later destroyed by numerical instability (c) because the chosen $h' = 0.002$ violates Eq. (43).

3.4 ARBBC splitting

By analogy with Eq. (12) and (36), the ARBBC splitting (14) is related to the evolution matrix

$$\mathcal{M} = \frac{2}{3} \left(e^{\frac{i\phi}{2}\mathbf{J}} e^{\frac{i\varepsilon}{2}\mathbf{K}} e^{\frac{i\phi}{2}\mathbf{J}} e^{\frac{i\varepsilon}{2}\mathbf{K}} + e^{\frac{i\varepsilon}{2}\mathbf{K}} e^{\frac{i\phi}{2}\mathbf{J}} e^{\frac{i\varepsilon}{2}\mathbf{K}} e^{\frac{i\phi}{2}\mathbf{J}} \right) - \frac{1}{6} \left(e^{i\phi\mathbf{J}} e^{i\varepsilon\mathbf{K}} + e^{i\varepsilon\mathbf{K}} e^{i\phi\mathbf{J}} \right),$$

with

$$\begin{aligned} \det \mathcal{M} &= 1 - \frac{2\eta^2}{9} (1 - \cos \phi + 2\varepsilon \sin \phi) + \frac{4\eta^4}{9}, \\ \text{Tr } \mathcal{M} &= 2(\cos \phi - \varepsilon \sin \phi) + \frac{4\eta^2}{3}, \end{aligned} \quad (46)$$

where we recall that $\eta = \varepsilon \sin(\phi/2)$.

By expanding $\det \mathcal{M}$ and $\text{Tr } \mathcal{M}$ in the vicinity of $\phi = \pm\pi$ and applying the root conditions from Fig. 1, we deduce that numerical stability is ensured when

$$\phi \in \begin{cases} (-\pi - \frac{2\varepsilon}{3}, \pi - \frac{4\varepsilon}{3}), & \varepsilon > 0, \\ (-\pi - \frac{4\varepsilon}{3}, \pi - \frac{2\varepsilon}{3}), & \varepsilon < 0, \end{cases} \quad (47)$$

cf., the conditions at the bottom of Fig. 2. The sufficient criterion (38) is then replaced by

$$|\phi| \leq \pi - \frac{4|\varepsilon|}{3}. \quad (48)$$

In practical terms, Eq. (48) means that to a good approximation Eq. (39) also applies to the ARBBC splitting, which is confirmed by numerical experiments similar to those from the previous sections.

Consider, for example, GNLSE of the form

$$i\partial_z \psi - \frac{\beta_2}{2} \partial_\tau^2 \psi + \frac{\beta_4}{24} \partial_\tau^4 \psi + \gamma |\psi|^2 \psi = 0, \quad (49)$$

with $\beta_2 \gamma > 0$. If Eq. (49) is carelessly reduced to the standard NLSE (44), the continuous wave solution (20) appears to be stable, but the stability is destroyed by a negative β_4 term, see [40, 41, 42, 43]. In fiber optics, this situation is sometimes called four-wave mixing instability [38].

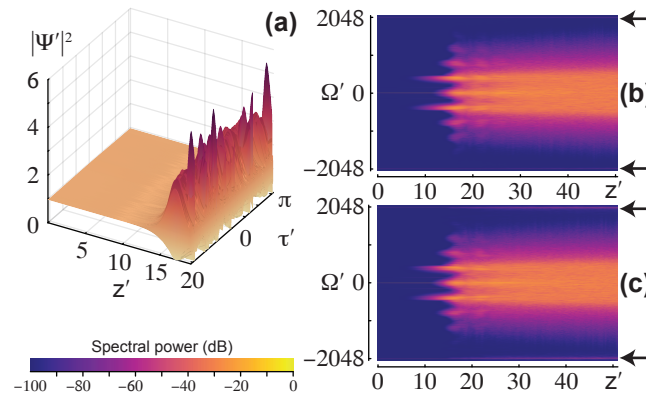


Figure 6: Normalized representation of the power $|\psi(z, \tau)|^2$ (the 3D plot) and the spectral power $|\tilde{\psi}(z, \Omega)|^2$ (density plots) that describes numerical solutions of Eq. (49) by ARBBC splitting. The parameters are given in Eq. (50). The onset of the four-wave mixing instability is shown in (a). It is also calculated in the presence of two small seed waves at $\Omega' = \pm 1973$ indicated by arrows in (b,c). The evolution step in (b) satisfies Eq. (47) and the seed waves do not grow. For the calculation in (c), Eq. (47) is violated and the numerical instability is developing, although very slowly.

Following Eq. (41), the normalized Eq. (49) depends on $\beta'_j = (2\pi)^j \beta_j / (T^j |\gamma| P_0)$ with $j = 2, 4$. The MI condition (29) reduces to $\frac{1}{2} \beta'_2 \Omega'^2 + \frac{1}{24} \beta'_4 \Omega'^4 \in (-2, 0)$. Specifically, we consider the following parameters

$$h' = 0.004, \quad \gamma' = 1, \quad \beta'_2 = 9 \cdot 10^{-7}, \quad \beta'_4 = -10^{-9}, \quad N = 2^{12},$$

$$\psi'|_{z'=0} = 1 + (\text{random signal}), \quad (50)$$

noise amplitude is 10^{-6} . Equation (48) requires $h' < 0.0043$, which is satisfied.

Figure 6a shows the onset of the four-wave mixing instability. Figure 6b, gives the spectral picture, the initial condition in this calculation was modified by two small seed waves located at $\Omega' = \pm 1973$. The seed waves, which are indicated by arrows, are not growing. Now we perform the same calculation for the overcritical $h' = 0.005$, which makes the additional seed waves unstable in accord with Eq. (47). The numerical instability is recognized in Fig. 6c. However, the instability, which is present where expected, is much less pronounced than in the previous calculations.

Last but not least, in the case of ARBBC splitting we face a new numerical instability. Indeed, expanding Eq. (46) at $\phi = 0$, we get

$$\det \mathcal{M} \Big|_{\phi=O(\varepsilon)} = 1 + O(\varepsilon^4) \quad \text{and} \quad \text{Tr} \mathcal{M} \Big|_{\phi=O(\varepsilon)} = 2 - \phi(\phi + 2\varepsilon) + O(\varepsilon^4).$$

The root conditions give the MI domain (31). However, a more accurate expansion of $\det \mathcal{M}$ in Eq. (46) yields

$$\det \mathcal{M} \Big|_{\phi=O(\varepsilon)} = 1 - \varepsilon^2 \phi^3 (\phi + 4\varepsilon) / 36 + O(\varepsilon^8),$$

such that $|\det \mathcal{M}| > 1$ for $\phi(\phi + 4\varepsilon) < 0$. This indicates the existence of numerical instability, its domain overlaps the MI domain (31). Although such numerical instability is always present, its increment is extremely small. We were unable to identify a single instance in which the effect of this instability was observed. Although we cannot rigorously prove this, it appears that this numerical instability can be disregarded without any risk.

4 Conclusions

In conclusion, we have studied the restrictions on the numerical integration step h that provide a numerically stable split-step solution of the GNLSE (19). We used the technique originally developed for NLSE and for the simplest Lie-Trotter splitting [29] and subsequently extended to GNLSE and to various multiplicative splittings [30, 31, 32, 33, 34]. The technique has been applied here to three additive splittings (12)–(14), which are of interest because different threads of such splitting schemes can be computed independently on a multi-core machine.

The main idea is to study the fundamental problem of continuous wave stability directly for the splitting method in question and then to compare the output with the well-known results based on GNLSE. The fundamental fact is that both multiplicative and additive splitting schemes can lead to numerical instabilities, which tend to disappear with the decrease of h . This is how the limitation of the integration step appears.

The second Strang splitting [7] is numerically unstable for any h . The splitting reported by Burstein and Mirin [13] requires, roughly speaking, a two times smaller integration step than the multiplicative splittings. The additive splitting proposed in Ref. [14] can be used with the same integration step as the multiplicative splittings. With a small correction, the critical step is given by Eq. (39). The latter criterion should be an integral part of any implementation of splitting solvers for GNLSE. This is especially important when the dispersion function in Eq. (16) and therefore the differential operator in GNLSE are approximated by a higher-order polynomial.

References

- [1] R.I. McLachlan and R. Quispel. Splitting methods. *Acta Numerica*, 11:341–434, January 2002.
- [2] W. Hundsdorfer and J. Verwer. *Numerical solution of time-dependent advection-diffusion-reaction equations*. Springer, 2003.
- [3] E. Hairer, C. Lubich, and G. Wanner. *Geometric Numerical Integration. Structure-Preserving Algorithms for Ordinary Differential Equations*, volume 31 of *Springer Series in Computational Mathematics*. Springer, Berlin, 2 edition, 2006.
- [4] H. Holden, K. Karlsen, K.-A. Lie, and H. Risebro. *Splitting methods for partial differential equations with rough solutions. Analysis and Matlab programs*. European Mathematical Society, Zürich, 2010.
- [5] Roland Glowinski, Stanley J. Osher, and Wotao Yin, editors. *Splitting Methods in Communication, Imaging, Science, and Engineering*. Scientific Computation. Springer, Berlin, 2016.
- [6] S. Buchholz, L. Gauckler, V. Grimm, M. Hochbruck, and T. Jahnke. Closing the gap between trigonometric integrators and splitting methods for highly oscillatory differential equations. *IMA Journal of Numerical Analysis*, 38(1):57–74, January 2018.
- [7] G. Strang. Accurate partial difference methods I: Linear Cauchy problems. *Arch. Rat. Mech. Anal.*, 12(1):392–402, January 1963.
- [8] G. Strang. On the construction and comparison of difference schemes. *SIAM J. Numer. Anal.*, 5(3):506–517, September 1968.

- [9] M. Suzuki. Fractal decomposition of exponential operators with applications to many-body theories and Monte Carlo simulations. *Phys. Lett. A*, 146(6):319–323, June 1990.
- [10] H. Yoshida. Construction of higher order symplectic integrators. *Phys. Lett. A*, 150(5-7):262–268, November 1990.
- [11] S. Blanes and P. C. Moan. Practical symplectic partitioned Runge-Kutta and Runge-Kutta-Nyström methods. *Journal of Computational and Applied Mathematics*, 142(2):313–330, May 2002.
- [12] W. Auzinger, H. Hofstätter, and O. Koch. Coefficients of various splitting methods. www.othmar-koch.org/splitting/.
- [13] S. Z. Burstein and A. A. Mirin. Third order difference methods for hyperbolic equations. *J. Comput. Phys.*, 5(3):547–571, June 1970.
- [14] Sh. Amiranashvili, M. Radziunas, U. Bandelow, K. Busch, and R. Čiegis. Additive splitting methods for parallel solutions of evolution problems. *Journal of Computational Physics*, 436(110320):1–14, July 2021.
- [15] A. Štikonas. The root condition for polynomial of the second order and a spectral stability of finite-difference schemes for Kuramoto-Tsuzuki equation. *Mathematical Modelling and Analysis*, 3(1):214–226, December 1998.
- [16] T.R. Taha and M.I. Ablowitz. Analytical and numerical aspects of certain nonlinear evolution equations. II. Numerical, nonlinear Schrödinger equation. *Journal of Computational Physics*, 55(2):231–253, August 1984.
- [17] Martino Lovisetto, Didier Clamond, and Bruno Marcos. Integrating factor techniques applied to the Schrödinger-like equations. Comparison with Split-Step methods. *Applied Numerical Mathematics*, 197:258–271, March 2024.
- [18] G. B. Whitham. *Linear and nonlinear waves*. John Wiley & Sons, New York, 1974.
- [19] R. W. Boyd. *Nonlinear Optics*. Academic, New York, 3 edition, 2008.
- [20] J. M. Dudley, G. Genty, and S. Coen. Supercontinuum generation in photonic crystal fiber. *Rev. Mod. Phys.*, 78(4):1135–1184, 2006.
- [21] K. E. Oughstun and H. Xiao. Failure of the quasimonochromatic approximation for ultrashort pulse propagation in a dispersive, attenuative medium. *Phys. Rev. Lett.*, 78(4):642–645, 1997.
- [22] A. H. Nayfeh. *Perturbation methods*. Wiley, 1973.
- [23] G. P. Agrawal. *Nonlinear Fiber Optics*. Academic, New York, 4 edition, 2007.
- [24] T. Brabec and F. Krausz. Nonlinear optical pulse propagation in the single-cycle regime. *Phys. Rev. Lett.*, 78(17):3282–3285, 1997.
- [25] P. Kinsler. Optical pulse propagation with minimal approximations. *Phys. Rev. A*, 81(1):013819, January 2010.
- [26] M. Kolesik, P. Jakobsen, and J. V. Moloney. Quantifying the limits of unidirectional ultrashort optical pulse propagation. *Phys. Rev. A*, 86(3):035801, September 2012.

- [27] L.N. Trefethen. *Spectral Methods in MATLAB*. SIAM, Philadelphia, 2000.
- [28] T. I. Lakoba. Long-time simulations of nonlinear Schrödinger-type equations using step size exceeding threshold of numerical instability. *J Sci Comput*, 72(1):14–48, July 2017.
- [29] J. A. C. Weideman and B. M. Herbst. Split-step methods for the solution of the nonlinear Schrödinger equation. *SIAM J. Numer. Anal.*, 23(3):485–507, June 1986.
- [30] T. I. Lakoba. Instability analysis of the split-step Fourier method on the background of a soliton of the nonlinear Schrödinger equation. *Numerical Methods for Partial Differential Equations*, 28(2):641–669, March 2012.
- [31] T. I. Lakoba. Instability of the split-step method for a signal with nonzero central frequency. *J. Opt. Soc. Am. B*, 30(12):3260–3271, December 2013.
- [32] F. Severing, U. Bandelow, and Sh. Amiranashvili. Spurious four-wave mixing processes in generalized nonlinear schrödinger equations. *J. Lightwave Technol.*, 41(16):5359–5365, August 2023.
- [33] J. Yang. *Nonlinear Waves in Integrable and Nonintegrable Systems*. SIAM, 2010.
- [34] Sh. Amiranashvili and R Čiegis. Stability of the higher-order splitting methods for the nonlinear Schrödinger equation with an arbitrary dispersion operator. *Mathematical Modelling and Analysis*, 29(3):560–574, 2024.
- [35] V. E. Zakharov and L. A. Ostrovsky. Modulation instability: the beginning. *Physica D: Nonlinear Phenomena*, 238(5):540–548, March 2009.
- [36] A. Hasegawa and M. Matsumoto. *Optical Solitons in Fibers*. Springer, 2003.
- [37] M. Erkintalo, K. Hammani, B. Kibler, C. Finot, N. Akhmediev, J. M. Dudley, and G. Genty. Higher-order modulation instability in nonlinear fiber optics. *Phys. Rev. Lett.*, 107(25):253901, Dec 2011.
- [38] M. Yu, C. J. McKinstrie, and G. P. Agrawal. Modulational instabilities in dispersion-flattened fibers. *Phys. Rev. E*, 52(1):1072–1080, July 1995.
- [39] A. Blanco-Redondo, C. M. de Sterke, J. E. Sipe, T. F. Krauss, B. J. Eggleton, and C. Husko. Pure-quartic solitons. *Nat. Commun.*, 7(10427):1–9, January 2016.
- [40] K. Kitayama, K. Okamoto, and H. Yoshinaga. Extended four-photon mixing approach to modulational instability. *J. Appl. Phys.*, 64(11):6586–6587, December 1988.
- [41] S. B. Cavalcanti, J. C. Cressoni, H. R. da Cruz, and A. S. Gouveia-Neto. Modulation instability in the region of minimum group-velocity dispersion of single-mode optical fibers via an extended nonlinear Schrödinger equation. *Phys. Rev. A*, 43(11):6162–6165, June 1991.
- [42] S. Pitois and G. Millot. Experimental observation of a new modulational instability spectral window induced by fourth-order dispersion in a normally dispersive single-mode optical fiber. *Opt. Commun.*, 226(1–6):415–422, October 2003.
- [43] J. D. Harvey, R. Leonhardt, S. Coen, G. K. L. Wong, J. C. Knight, W. J. Wadsworth, and P. St. J. Russell. Scalar modulation instability in the normal dispersion regime by use of a photonic crystal fiber. *Opt. Lett.*, 28(22):2225–2227, November 2003.